OPEN ACCESS
IOP Publishing
Journal of Physics B: Atomic, Molecular and Optical Physics
J. Phys. B: At. Mol. Opt. Phys. **47** (2014) 204024 (6pp)
doi:10.1088/0953-4075/47/20/204024

Tunnelling time in strong field ionisation

Alexandra S Landsman and Ursula Keller

Physics Department, ETH Zurich, CH-8093 Zurich, Switzerland

E-mail: landsmanster@gmail.com

Received 23 June 2014, revised 29 July 2014
Accepted for publication 29 July 2014
Published 8 October 2014

Abstract

We revisit the common approaches to tunnelling time in the context of attoclock experiments. These experiments measure tunnelling time using close-to-circularly polarised light of the infrared ultrashort laser pulse. We test the sensitivity of the attoclock measurements of tunnelling time to non-adiabatic effects, as described by a well-known theoretical model first developed by Perelomov, Popov, and Terent'ev. We find that in the case of ionisation of helium, both adiabatic and non-adiabatic theories give very similar predictions for ionisations times over a wide intensity range typical of ultrafast experiments.

Keywords: tunnelling, strong field ionisation, attoclock experiments

(Some figures may appear in colour only in the online journal)

1. Introduction

While tunnelling probabilities and escape rates are well defined and widely accepted [1–3], the question of how long it takes a particle to transverse a barrier has been the subject of intense theoretical debate for decades. Since MacColl [4], there have been repeated attempts to address this question with 'no clear consensus, however, about the existence of a simple expression for this time, and the exact nature of that expression' [5]. To complicate matters, the tunnelling time itself is not well defined. Different definitions exist, arguably related to different and complementary aspects of the tunnelling problem and depending on the experimental context. An excellent review of these different definitions and the various theoretical difficulties arising in approaching tunnelling time are given, for example, in [5].

In this paper, we will revisit these various definitions of tunnelling time in the context of attoclock measurements of strong field tunnel ionisation times [6]. The attoclock uses close-to-circular polarisation to time various processes in strong field ionisation with attosecond precision. For a detailed description of how the attoclock works, we refer the reader to prior publications [6–8]. Here, we focus on how strong field ionisation theory is used to extract *experimentally* determined tunnelling times from the attoclock experiments.

Note, these theoretical models were developed in the context of strong field ionisation and are quite independent of different definitions of tunnelling time also discussed here. Hence, this work addresses the tunnelling time question from both ends, bringing the various approaches to tunnelling time developed outside the context of strong field ionisation together with strong field ionisation theory, developed quite independently of the tunnelling time question. It is hoped that this approach will benefit both fields.

The rest of the paper is organised as follows. First, we describe a path integral approach to the tunnelling time problem, showing how a probability amplitude of tunnelling times can be constructed using this approach. We will then relate this path integral formulation to the four widely used definitions of tunnelling time: the Büttiker–Landauer, the Eisenbud–Wigner, the Pollack–Miller, and the Larmor time. We will then discuss how tunnelling times are extracted from the attoclock measurements. We find that for typical experimental intensities and ionisation of helium gas, the most commonly used models of strong field ionisation, namely the semiclassical two-step model [9, 10] and the imaginary time method (introduced by Perelomov, Popov, and Terent'ev (PPT) [3]) give very similar predictions for tunnelling time.

2. Feynman path integral formulation for tunnelling time

In this section, we give an overview of the Feynman path integral formulation for tunnelling time. This approach has two advantages. First, it lends to a derivation of a probability amplitudes of tunnelling times, rather than a deterministic tunnelling time [11]. It has, for instance, been argued by Yamada that the range of possible tunnelling times for an opaque barrier is so broad that 'a unique tunnelling time cannot be considered even in a loose sense' [12]. Second, the path integral approach provides a convenient and informative way to unify four of the commonly used definitions of tunnelling time [5, 13, 14].

2.1. General derivation

Here we summarise the path integral approach for the calculation of the tunnelling time amplitude. More detail can be found in [11]. The Feynman path integral formulation [16, 17] has the advantage of expressing the total wavefunction $\Psi(x, T)$ as a sum over all 'possible' paths, with each path contributing $\exp[\mathrm{i}S[x''(t)]]$, where $S[x''(t)]$ is the action for a particular path $x''(t)$ with endpoints: $x''(0) = x''$ and $x''(T) = x$,

$$S\left[x''(t)\right] = \int_0^T \left[\left(m\dot{x}''\right)^2 \Big/ 2m - V\left(x''\right)\right]\mathrm{d}t \tag{1}$$

The total wavefunction is then given by [16],

$$\Psi(x, T) = \int \mathrm{d}x' \int Dx''(t) \exp\left[\mathrm{i}S\left[x''(t)\right]\Big/\hbar\right]\Psi(x', 0) \tag{2}$$

Since each path is deterministic, it is possible to associate with each $x''(t)$ a time that it spends inside the barrier region. The idea is then to separate the paths that spend an exact amount of time τ inside of the barrier, resulting in a wavefunction composed only of these paths,

$$\Psi(x, T|\tau) = \int \mathrm{d}x' \int Dx''(t)\delta\left(t_b\left[x''(t)\right] - \tau\right) \times \exp\left(\mathrm{i}S\left[x''(t)\right]/\hbar\right)\Psi(x', 0) \tag{3}$$

where $t_b[x''(t)]$ is the time spent inside of the barrier region by $x''(t)$. Note that the barrier transversal time here is well defined since $x''(t)$ is deterministic, with t_b given by [5],

$$t_b[x(t)] = \int_0^T \Theta(x(t))\mathrm{d}t \tag{4}$$

where $\Theta(x(t)) = 1$ for $x_0 \leqslant x(t) \leqslant x_e$, and is equal to zero otherwise. Here, x_0 and x_e are the entrance and the exit points of the tunnel, respectively. Equation (4) gives the resident (dwell) time, or the time a particle spends inside the barrier region.

It has been shown that the wavefunction in equation (3) satisfies the following 'clocked' Schrödinger equation [15],

$$\mathrm{i}\hbar\frac{\partial\Psi(x, t|\tau)}{\partial t} = -\frac{\hbar^2}{2m}\frac{\partial^2\Psi(x, t|\tau)}{\partial x^2} + V(x)\Psi(x, t|\tau) - \mathrm{i}\hbar\Theta(x)\frac{\partial\Psi(x, t|\tau)}{\partial\tau} \tag{5}$$

From equation (3), it is clear that the total wavefunction can be expressed as an integral sum of the $\Psi(x, T|\tau)$ wavefunctions,

$$\Psi(x, T) = \int_0^\infty \Psi(x, T|\tau)\mathrm{d}\tau \tag{6}$$

Therefore, the total wavefunction is the sum of the interfering wavefunctions that corresponds to the amount τ that the particle spends traversing a barrier, much like the interference pattern in a double-slit experiment is composed of wavefunctions going through each slit.

The relation in equation (3) has been expressed in propagator form as [5, 13],

$$G_\tau(k_0, x_e, x_0) = t\left(k_0, V|\tau\right)G_0\left(k_0, x_e, x_0\right) = \int_{-\infty}^\infty \mathrm{d}t\mathrm{e}^{\mathrm{i}E_0t/\hbar}\int_{x(0)=x_0}^{x(T)=x_e} Dx''(t) \times \delta\left(t_b\left[x''(t)\right] - \tau\right)\mathrm{e}^{\mathrm{i}S\left[x''(t)\right]/\hbar} \tag{7}$$

where $t\left(k_0, V|\tau\right)$ is the contribution of paths spending time τ inside the barrier to the transmission amplitude $t(k_0, V)$ [13], and $G_0\left(k_0, x_e, x_0\right)$ is the propagator in the absence of a barrier. The total transmission amplitude is given by: $t\left(k_0, V\right) = \int_{-\infty}^\infty t\left(k_0, V|\tau\right)\mathrm{d}\tau$

The δ function in equations (3) and (7) can be written in the following form:

$$\delta\left(t_b\left(x''\right) - \tau\right) = \frac{1}{2\pi\hbar}\int_{-\infty}^\infty \mathrm{d}W\exp^{-\mathrm{i}W\left[t_b\left(x''\right)-\tau\right)/\hbar]} \tag{8}$$

Substituting equation (8) into equation (7) and using equations (1) and (4), we see that each term in equation (8) is equivalent to adding a rectangular potential of height $W\Theta(x)$ to $V(x)$. If we denote the transmission amplitude in the presence of the potential $W\Theta(x) + V(x)$ by $t(k_0, V + W)$, equation (7) becomes [11, 13]:

$$t\left(k_0, V|\tau\right) = \frac{1}{2\pi\hbar}\int_{-\infty}^\infty \mathrm{d}W\exp^{\mathrm{i}W\tau/\hbar}t\left(k_0, V + W\right) \tag{9}$$

Each $t(k_0, T|\tau)$ is a probability amplitude that a particle impinging on a barrier with energy E will spend time τ inside it before being transmitted. *This equation gives a prescription for calculating the part of the wavefunction that corresponds to a specific time τ that the electron spends inside the potential barrier before being transmitted.*

An alternative definition to the dwell or residence time given by equation (4) is the passage time, which corresponds to the difference between the last time a path left the barrier at x_e and the first time it entered at x_0. For the passage time, the

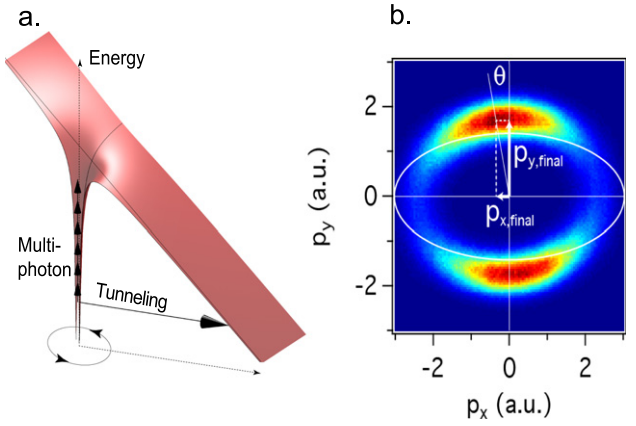

Figure 1. (a). The combined potential created by the Coulomb field of the atom and the laser field. (b) Electron momenta distributions measured at the detector after strong field ionization for close-to-circularly polarized light of ellipticity, $\epsilon = 0.87$.

amplitude in equation (9) is modified to [14]

$$t_p(k_0, V|\tau) = \frac{\hbar k_0}{2\pi m}\int_{-\infty}^{\infty} dk \exp^{-iE\tau/\hbar} t(k_0 + k, V) \quad (10)$$

It is tempting to think of $|t(k_0, V|\tau)|^2$ as a probability that a particle will spend an amount of time τ inside of the barrier before being transmitted. However, to quote Landauer: 'Now, there is little doubt that the propagator [in equation (7)] contains information about paths that traverse the barrier and spend a time τ in the process. But it is not clear what procedure is needed to calculate physical quantities with the Feynman approach.' [5] This has led to the different definitions of tunnelling time (see subsection 2.2), all of which can be expressed as various averages using the probability amplitude given in equations (9) and (10). However, due to the interference of the tunnelling time amplitudes, there is no obviously correct averaging procedure to use for calculation of expected tunnelling times. Formally, this means that the wavefunction $\Psi(x, T|\tau)$ does not satisfy the weak decoherence condition [12, 18] given by

$$ReD[\tau; \tau'] = \delta(\tau - \tau')P(\tau) \quad (11)$$

where $D[\tau; \tau']$ is the decoherence functional [18],

$$D[\tau; \tau'] = lim_{t\to\infty}\int_{x_e}^{\infty} dx \Psi^*(x, t|\tau)\Psi(x, t|\tau') \quad (12)$$

To calculate the probability distribution of tunnelling times, the amplitude is further coarse-grained to reflect the underlying uncertainty of the experimental measurement [11]:

$$\left\langle t(k_0, V|\tau)\right\rangle = \int_0^{\infty} t(k_0, V|\tau') e^{-(\tau-\tau')^2/\tau_0^2} d\tau' \quad (13)$$

where τ_0 in equation (13) is determined by the measurement. The coarse-grained unnormalised probability distribution is then given by $|\langle t(k_0, V|\tau)\rangle|^2$ and depends on the accuracy of the measuring device. It has been recently argued in [19] that the aforementioned coarse-grained probability amplitude satisfies the weak decoherence condition and therefore can be used to construct a probability distribution of tunnelling times.

2.2. Definitions of tunnelling time

In this subsection, we give an overview of the four well-known definitions of tunnelling time and show how they can all be viewed as arising from different averaging procedures using the tunnelling time probability amplitude presented in equations (9) and (10).

Four widely used definitions of tunnelling time are the **Larmor** time [20–22], τ_{LM}; the **Büttiker–Landauer** time [23], τ_{BL}; the **Eisenbud–Wigner** time [24], τ_{EW}; and the **Pollack–Miller** time [25], τ_{PM}. All of these times are based on very different models, but they can all be expressed in terms of the transmission amplitude: $T = |T|e^{i\theta}$, the height of the potential V, and the incident energy of the particle E. The first two times depend on the potential and have been called the *resident (or dwell) time* [14],

$$\tau_{BL} = -\hbar\partial\, ln\, |T|/\partial V; \qquad \tau_{LM} = -\hbar\partial\theta/\partial V \quad (14)$$

The Keldysh time, arising in strong field ionisation [2, 26], is a special case of the Büttiker–Landauer time, which was developed for arbitrary potential barriers. The other two times depend on the incident energy of the particle and have been called the *passage time*,

$$\tau_{PM} = \hbar\partial\, \ln\, |T|/\partial E; \qquad \tau_{EW} = \hbar\partial\theta/\partial E \quad (15)$$

For the Eisenbud–Wigner time, an additional term corresponding to propagation through the vacuum must be added to get the absolute value of tunnelling time [27].

While each of the four definitions of tunnelling times were developed independently and using different physical considerations, they have been unified within the path integral approach [28], as we now describe. The Larmor and the Büttiker–Landauer times can be expressed as the real and imaginary parts, respectively, of the complex quantity obtained when averaging with $t(k_0, V|\tau)$, given by equation (9):

$$\tau_{LM} - i\tau_{BL} = \frac{\int_0^{\infty} t(k_0, V|\tau)\tau d\tau}{\int_0^{\infty} t(k_0, V|\tau) d\tau} \quad (16)$$

where the denominator in the previous equation is for normalisation. Similarly, the Eisenbud–Wigner and the Pollack–Miller times are the real and imaginary parts (respectively) of averaging with $t_p(k_0, V|\tau)$, given by equation (10):

$$\tau_{EW} - i\tau_{PM} = \frac{\int_0^{\infty} t_p(k_0, V|\tau)\tau d\tau}{\int_0^{\infty} t_p(k_0, V|\tau) d\tau} \quad (17)$$

These four times, as well as the probability distribution of tunnelling times constructed using the path integral approach, were compared to the attoclock measurements in [40]. It was found that of these four times, only the Larmor time was within experimental uncertainty, excluding the other three tunnelling time definitions as being 'correct' for interpreting attoclock measurements. In addition, the probability distribution constructed using the path integral approach was found to be compatible with experimental results. Since, as mentioned earlier, the measured tunnelling time may well depend on the nature of the experiment, it is worthwhile to

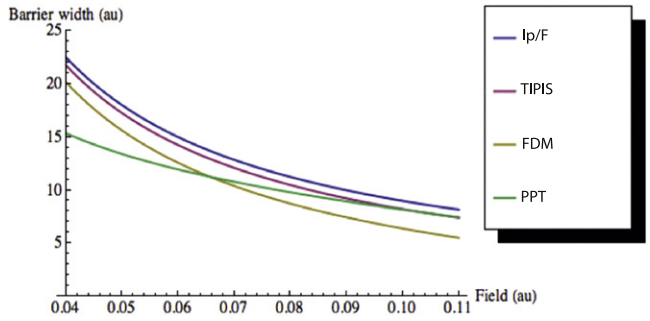

Figure 2. Approximate exit points predicted by different models: PPT, TIPIS, and FDM (field-direction model) for helium. The range of field strengths is comparable to that shown in figure 3, corresponding to intensities of $10^{14} - 8 \times 10^{14}$W cm^{-2}. The corresponding range of γ is also shown in figure 3. At high field strengths, corresponding to $\gamma \ll 1$, the PPT curve approaches the adiabatic short-range potential case, or the I_p/F curve.

examine in detail how this time is extracted from the attoclock measurement. This is done in the following section.

3. Attoclock measurements of tunnelling time

The principle of the attoclock has been described in some detail in prior publications (see, for example, [7, 8]). Here, we will only address the aspects of attoclock tunnelling time measurements that depend on strong field ionisation theory as described next. In particular, the attoclock experiment measures electron momenta distributions at the detector created by tunnel ionisation. Tunnel ionisation occurs when the strong field of the laser distorts the atomic potential, creating a barrier through which the electron can tunnel and be subsequently accelerated by the strong laser field (figure 1(a)) [2, 9, 29]. The final momentum of the electron is measured at the detector some time after the laser pulse has passed (figure 1(b)).

One common approach in analysing measured electron momenta distributions is to use a two-step semi-classical model, pioneered by Corkum [9], among others, in the early 1990s. The basic idea behind the two-step model is to treat the first step (tunnel ionisation) quantum mechanically, often using ADK probability distribution, named after Ammosov, Delone, and Krainov [1]. The second step is then treated classically, borrowing ideas from plasma physics, where electrons are assumed to be free and interacting classically with electric and magnetic fields. Further simplification results from the dipole approximation, which is valid at sufficiently low intensities and allows one to neglect magnetic field effects, which normally would considerably complicate the dynamics [30, 31]. The laser pulse can then be described as:

$$\mathbf{F}(t) = \frac{-F_0 f(t)}{\sqrt{\epsilon^2 + 1}}[\cos(\omega t + \phi_c)\hat{x} + \epsilon \sin(\omega t + \phi_c)\hat{y}] \quad (18)$$

where ω is the central frequency of the laser, ϵ is the ellipticity (the major axis of polarisation is along $\hat{x}$), and $f(t)$ is the slowly varying pulse envelope: $f_{\max} = f(0) = 1$. For many-cycle pulses, we can approximate the carrier-envelope offset (CEO) phase [32]: $\phi_c \approx 0$. In the following discussion, we shall set $\phi_c = 0$, corresponding to the peak of the electric field occurring at $t = 0$.

The electron momenta distributions obtained from ionisation with elliptically polarised ultra-short laser pulse, such as shown in figure 1(b), provide a wealth of information about the dynamics of tunnel ionisation [33]. In particular, the momenta spreads provide information about the dynamics at the tunnel exit [34–36] and Coulomb focusing [37]. The shifting of the centre of the electron momenta distribution with increasing ellipticity of laser light can be used to analyse the disappearance of Rydberg states [38, 39], as well as Coulomb focusing and Coulomb asymmetry [39].

Of particular importance to this work is the angle of the center of the electron momenta distribution. It is from this angle that experimentally measured tunnelling time $\tau_{\exp}$ is obtained [6–8, 10, 40]:

$$\tau_{\exp} = \frac{\theta_i}{\omega} = \frac{(\theta_m - \theta_{Coul} - \theta_{str})}{\omega} \quad (19)$$

where ω is the central frequency of the laser, θ_{Coul} is the Coulomb correction, θ_{str} is the (close to 90 degrees) streaking angle, and θ_m is the experimental observable given by:

$$\theta_m = \theta + \pi/2 \quad (20)$$

where θ is defined in figure 1(b). It is clear from figure 1(b) that θ, from which tunnelling time is extracted, depends on the final momenta of the centre of the electron momenta distribution in the plane of polarisation, or $p_{y,\text{final}}$ and $p_{x,\text{final}}$. Since $\tau_{\exp}$ is extracted by comparing measured θ to theoretical predictions, which determine θ_{Coul}, we examine next two theoretical models commonly used to calculate θ_{Coul}, namely the TIPIS model [10] and the stationary phase method, first pioneered by Perelomov, Popov, and Terent'ev (PPT) [3].

The TIPIS model is adiabatic, thereby predicting the most likely electron velocity at the tunnel exit to be zero. The exit point is given by the full solution of the Schrödinger equation in parabolic coordinates [10], which can be approximated as [36]:

$$x_{\text{tipis}} \approx \frac{I_p + \sqrt{I_p^2 - 4\beta F_{\max}}}{2F_{\max}} \quad (21)$$

where $\beta = 1 - \sqrt{2I_p}/2$, I_p is the ionisation potential and F_{max} is the peak electric field. The parabolic exit point has been used as an initial condition in the Classical Trajectory Monte Carlo (CTMC) simulations combined with the ADK probability distribution for the initial electron momenta to obtain electron momenta distributions, which were in good agreement with experimental data in [10].

An alternative to using the TIPIS model for initial conditions at the tunnel exit is to use a non-adiabatic model, pioneered by PPT [3], and subsequently developed by others [41]. Unlike the TIPIS model, PPT does not take account of a Coulomb potential while tunnelling. On the other hand, it accounts for non-adiabatic effects, determined by the Keldysh

parameter: $\gamma = \omega\sqrt{2I_p}/F_{\max}$. In this case, the initial most probable velocity at the tunnel exit is non-zero and is given by [41]:

$$\mathbf{p}_{na} = \frac{\epsilon F_0}{\omega\sqrt{\epsilon^2+1}}\left(\frac{\sinh(\tau_0)}{\tau_0} - 1\right)\hat{y} \tag{22}$$

Note that, in contrast to the adiabatic case, the momentum spread at the tunnel exit is centered around $\mathbf{p}_{na}$ rather than zero. The prefactor and the standard deviation are also somewhat larger, and can be found in [3, 41]. The exit point is also different from the adiabatic case, tending to $x_{na} \to I_p/F$ as $\gamma \to 0$:

$$x_{na} = \frac{F_{\max}}{\omega^2}\left(ch(\omega\tau_0) - 1\right) \tag{23}$$

where τ_0 solves the following equation [41]:

$$\sinh^2\tau_0\left[1 - \epsilon^2\left(\coth\tau_0 - \frac{1}{\tau_0}\right)^2\right] = \gamma^2 \tag{24}$$

The different exit points predicted by various models are shown in figure 2. From the figure, it is clear that over a large range of field strengths of the laser, the non-adiabatic PPT theory predicts a smaller exit point than the TIPIS model. At higher intensities, corresponding to $\gamma \ll 1$, the PPT prediction for the exit point approaches the case of short-range adiabatic potential, where the barrier width is I_p/F. Interestingly, it is possible for the non-adiabatic exit point predicted by PPT to be farther out than the TIPIS prediction for sufficiently high intensities. Also included in figure 2 is the so-called field direction model (FDM), which is not discussed here. More detail on FDM can be found, for example, in [10].

It is clear that the two models (TIPIS and PPT), by predicting different initial conditions at the tunnel exit, will result in different final momenta, $p_{y,\text{final}}$ and $p_{x,\text{final}}$ of the centre of the distribution at the detector. This is indeed the case. The prediction of $p_{y,\text{final}}$ from non-adiabatic theory is given by:

$$p^{N-A}_{y,\text{ final}} = C(\gamma)p^{A}_{y,\text{ final}} \tag{25}$$

where $C(\gamma) = \sinh(\tau_0)/\tau_0$, and $p^{N-A}_{y,\text{ final}}$ and $p^{A}_{y,\text{ final}}$ are non-adiabatic and adiabatic predictions, respectively. Since $C(\gamma) > 1$, the non-adiabatic momentum offset along the minor axis of polarisation is always greater than the corresponding adiabatic expression. Likewise, $p_{x,\text{final}}$ is different for the two cases because it is determined by the Coulomb correction, which is different in the adiabatic versus non-adiabatic case due to the different initial conditions at the tunnel exit predicted by the two theories.

The predictions for the Coulomb angle, θ_{Coul}, were calculated from CTMC simulations [34, 36, 42] using two different models: the TIPIS and the non-adiabatic PPT model, with initial conditions given by equations (21), (22), and (23). It was found that while the initial conditions at the tunnel exit become increasingly different at lower intensities, the difference in θ_{Coul} remains small for tunnel ionisation of helium, leading to similar predictions of tunnelling time, based on equation (19). This result is shown in figure 3.

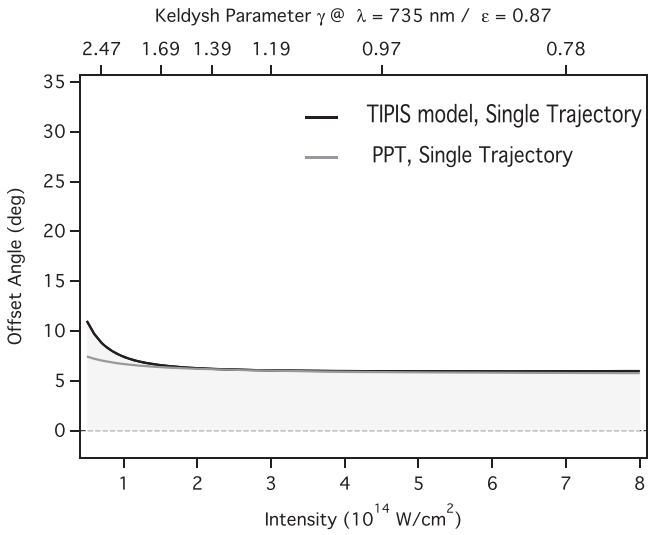

Figure 3. Comparison of adiabatic (TIPIS) versus non-adiabatic (PPT) predictions for the Coulomb correction, θ_{Coul}, for ionisation of helium over a wide intensity range.

The similar offset angle, θ_{Coul}, in spite of different initial conditions for adiabatic and non-adiabatic propagation in the continuum, can be understood by considering that both $p_{x,\text{final}}$ and $p_{y,\text{final}}$ are larger for the non-adiabatic versus adiabatic case, leading to similar ratios of $p_{x,\text{final}}/p_{y,\text{final}}$ and hence similar final angles, at least for ionisation of helium.

The offset angle, θ_{Coul}, is used to extract tunnelling time from experimental measurements, using equation (19), where θ_m is the experimentally measured angle and the streaking angle is given by:

$$\theta_{\text{str}} - \pi/2 \approx \frac{\left(1-\epsilon^2\right)}{\epsilon}\theta_i \tag{26}$$

This equation is, of course, not valid in the limit $\epsilon \to 0$, but is accurate in the high ellipticity regime, where the attoclock operates. The previous equation, combined with θ_{Coul}, shown in figure 3 for two different theories, allows the calculation of experimental tunnelling time, τ_{exp}, in accordance with equation (19).

This experimentally extracted time, τ_{exp}, was compared to five different theoretical values in figure 3 of [40]. The Keldysh time, given by $\tau_{\text{Kel}} = \gamma/\omega$, corresponds to the Büttiker–Landauer time (within the WKB and the short-range potential approximations), which in turn is given by the red curve in figure 3 of [40]. Therefore, the Keldysh time, as well as Eisenbud–Wigner and the Pollack–Miller times, fall significantly outside the attoclock experimental determination of tunnelling time, also given in figure 3 of [40].

The estimates of the average velocity can also be made from theoretical values as well as the experimental data presented in [40]. Let us compare these values to the Keldysh under-barrier electron velocity, which is given by $v_{\text{Kel}} = I_p/\left(F_{\max}\tau_{\text{Kel}}\right)$. The Pollack–Miller and the Büttiker–Landauer average under-barrier velocity are comparable to v_{Kel}, since the tunnelling times are comparable. On the other

hand, $v_{EW} \approx 2v_{Kel}$, while the Larmor velocity, the velocity arising from the FPI approach, as well as the experimentally determined velocity, are less than 10 percent of v_{Kel}.

4. Conclusion

We have discussed important theoretical definitions of tunnelling time, developed outside ultrafast physics, in the context of attoclock experiments performed using an ultrafast laser pulse. For proper comparison of experimental results with various theoretical predictions, we focused on the sensitivity of the attoclock measurements to the underlying strong field ionisation model used to extract tunnelling time. In particular, we compared experimental tunnelling time obtained using non-adiabatic PPT and adiabatic TIPIS models.

We found that for a wide range of experimental intensities, non-adiabatic PPT theory agrees with the adiabatic model for the final offset angle of the centre of electron momenta distribution after strong field ionisation of helium. Our results have implications for extraction of tunnelling time from the attoclock experiments [6, 40], suggesting that although non-adiabatic theories predict significantly different initial conditions at lower intensities, the effect on the tunnelling time estimate for ionisation of helium is small. This further confirms that three of the commonly used tunnelling times, namely the Büttiker–Landauer, the Pollack–Miller, and the Eisenbud–Wigner time (see equations (14) and (15)), are incompatible with the attoclock measurements.

Further directions of research include the role of the four times described here in ultrafast laser experiments. For instance, it is possible that the Büttiker–Landauer time, closely related to Keldysh time, is the correct time for the build-up of a steady-state tunnelling flux. This would be in agreement with results in [26]. Alternatively, the Büttiker–Landauer time can be shown to correspond to the imaginary part of the tunnelling time [43]. In this case, the physical interpretation of the Büttiker–Landauer time, as well as a related Pollack–Miller time, remains an open problem.

The analytical connection between the four theoretical times discussed here is well known and well described using the Feynman path integral approach, as can be seen in equations (16) and (17). However, the physical connection between these four times remains a fascinating open question which can be further explored in the context of experimental ultrafast science.

Acknowledgments

We thank R Boge, C Hofmann, and C Cirelli for discussions and assistance in preparing the figures. This research was supported by the ERC advanced grant, NCCR MUST, funded by the Swiss National Science Foundation (SNSF), and an SNSF project grant. Our ultrafast activities are supported by the ETH Femtosecond and Attosecond Science and Technology (ETH-FAST) initiative as part of the NCCR MUST program.

References

[1] Ammosov M V, Delone N B and Krainov V P 1986 *Sov. Phys. JETP* **64** 1191
[2] Keldysh L V 1965 *JETP* **20** 1307
[3] Perelomov A M, Popov V S and Terent'ev M V 1966 *JETP* **50** 1393
[4] MacColl L A 1932 *Phys. Rev.* **40** 621
[5] Landauer R and Martin Th 1994 *Rev. Mod. Phys.* **66** 217
[6] Eckle P *et al* 2008 *Science* **322** 1525
[7] Pfeiffer A N, Cirelli C, Smolarski M and Keller U 2013 *Chem. Phys.* **414** 84
[8] Gallmann L, Cirelli C and Keller U 2012 *An. Rev. Phys. Chem.* **63** 447
[9] Corkum P B 1993 *Phys. Rev. Lett.* **71** 1994
[10] Pfeiffer A N, Cirelli C, Smolarski M, Dimitrovsky D, Mahmoud A, Madsen L and Keller U 2011 *Nat. Phys.* **7** 428
[11] Sokolovski D, Brouard S and Connor J N L 1994 *Phys. Rev.* A **50** 1240
[12] Yamada N 1999 *Phys. Rev. Lett.* **83** 3350
[13] Fertig H A 1990 *Phys. Rev. Lett.* **65** 2321
[14] Yamada N 2004 *Phys. Rev. Lett.* **93** 170401
[15] Sokolvski D 1997 *Phys. Rev. Lett.* **79** 4946
[16] Feynman R P and Hibbs A R 1965 *Quantum Mechanics and Path Integrals* (New York: McGraw-Hill)
[17] Feynman R 1989 *The Feynman Lectures on Physics* (Boston, MA: Addison-Wesley)
[18] Hartle J B 1991 *Proc. of the 25th Int. Conf. on High Energy Physics* (Singapore: World Scientific)
[19] Boonchui S and Sa-yakanit V 2008 *Phys. Rev.* A **77** 044101
[20] Baz' A I 1967 *Sov. J. Nucl. Phys.* **4** 182
[21] Rybachenko V F 1967 *Sov. J. Nucl. Phys.* **5** 635
[22] Buttiker M 1983 *Phys. Rev.* B **27** 6178
[23] Buettiker M and Landauer R 1982 *Phys. Rev. Lett.* **49** 1739
[24] Wigner E P 1955 *Phys. Rev.* **98** 145
[25] Pollak E and Miller W H 1984 *Phys. Rev. Lett.* **53** 115
[26] McDonald C R, Orlando G, Vampa G and Brabec T 2013 *Phys. Rev. Lett.* **111** 090405
[27] Hauge E H and Stovneng J A 1989 *Rev. Mod. Phys.* **61** 917
[28] Sokolovski D and Baskin L M 1987 *Phys. Rev.* A **36** 4606
[29] Krausz F and Ivanov M 2009 *Rev. Mod. Phys.* **81** 163
[30] Landsman A S, Cohen S A and Glasser A H 2004 *Phys. Plasmas* **11** 947
[31] Quere F 2009 *Nat. Phys.* **5** 93
[32] Telle H R *et al* 1999 *Appl. Phys.* B **69** 327
[33] Ooi C H, Ho W and Bandrauk A D 2012 *Phys. Rev.* A **86** 023410
[34] Pfeiffer A N, Cirelli C, Landsman A S, Smolarski M, Dimitrovsky D, Madsen L and Keller U 2012 *Phys. Rev. Lett.* **109** 083002
[35] Arissian L, Smeenk C, Turner F, Trallero C, Sokolov A V, Villeneuve D M, Staudte A and Corkum P B 2010 *Phys. Rev. Lett.* **105** 133002
[36] Hofmann C, Landsman A S, Cirelli C, Pfeiffer A N and Keller U 2013 *J. Phys. B: At. Mol. Opt. Phys.* **46** 125601
[37] Shafir D *et al* 2013 *Phys. Rev. Lett.* **111** 023005
[38] Landsman A S, Pfeiffer A N, Hofmann C, Smolarski M, Cirelli C and Keller U 2013 *New J. Phys.* **15** 013001
[39] Landsman A S, Hofmann C, Pfeiffer A N, Cirelli C and Keller U 2013 *Phys. Rev. Lett.* **111** 263001
[40] Landsman *et al* 2013 arxiv:1301.2766
[41] Mur V D, Popruzhenko S V and Popov V S 2001 *J. Exp. Theor. Phys.* **92** 777
[42] Boge R, Cirelli C, Landsman A S, Heuser S, Ludwig A, Maurer J, Weger M, Gallmann L and Keller U 2013 *Phys. Rev. Lett.* **111** 103003
[43] Zhao J and Lein M 2013 *Phys. Rev. Lett.* **111** 043901